THE COMPANY OF
Biologists

RESEARCH ARTICLE

LRP2 mediates folate uptake in the developing neural tube

Esther Kur[1],[*],[‡], Nora Mecklenburg[1],[‡], Robert M. Cabrera[2], Thomas E. Willnow[1] and Annette Hammes[1],[§]

ABSTRACT

The low-density lipoprotein (LDL) receptor-related protein 2 (LRP2) is a multifunctional cell-surface receptor expressed in the embryonic neuroepithelium. Loss of LRP2 in the developing murine central nervous system (CNS) causes impaired closure of the rostral neural tube at embryonic stage (E) 9.0. Similar neural tube defects (NTDs) have previously been attributed to impaired folate metabolism in mice. We therefore asked whether LRP2 might be required for the delivery of folate to neuroepithelial cells during neurulation. Uptake assays in whole-embryo cultures showed that LRP2-deficient neuroepithelial cells are unable to mediate the uptake of folate bound to soluble folate receptor 1 (sFOLR1). Consequently, folate concentrations are significantly reduced in $Lrp2^{-/-}$ embryos compared with control littermates. Moreover, the folic-acid-dependent gene *Alx3* is significantly downregulated in *Lrp2* mutants. In conclusion, we show that LRP2 is essential for cellular folate uptake in the developing neural tube, a crucial step for proper neural tube closure.

KEY WORDS: LRP2, Embryonic development, Endocytic receptor, Folate, Folate receptor, Neural tube closure defects

INTRODUCTION

The low-density lipoprotein (LDL) receptor-related protein 2 (LRP2), also known as megalin (Saito et al., 1994), is a multifunctional cell-surface receptor that is structurally related to the LDL receptor (Nykjaer and Willnow, 2002). Endocytosis through LRP2 is important for the efficient uptake of several vitamins and hormones bound to their carrier proteins. Examples are the re-uptake of vitamin D and retinol from the primary urine (Christensen et al., 1999; Nykjaer et al., 1999), as well as the uptake of androgens and estrogens into steroid-responsive cells (Hammes et al., 2005).

LRP2 plays a crucial role in forebrain development. The receptor is highly expressed in the neuroepithelium and loss of receptor activity in the developing central nervous system (CNS) in gene-targeted mice causes holoprosencephaly (HPE), a failure of the forebrain hemispheres to separate along the midline (Spoelgen et al., 2005; Willnow et al., 1996). Patients with

autosomal recessive *LRP2* gene defects suffer from Donnai-Barrow syndrome, a disorder associated with forebrain anomalies (Kantarci et al., 2007). We previously clarified the molecular mechanism underlying the HPE phenotype by identifying LRP2 as a novel component of the sonic hedgehog (SHH) signaling machinery in the ventral forebrain neuroepithelium (Christ et al., 2012). LRP2 deficiency in mice leads to failure of the neuroepithelium to respond to SHH and, consequently, to improper specification of structures of the ventral forebrain midline.

Besides the HPE phenotype, we have also noted additional cranial neural tube defects (NTDs) in LRP2-deficient mice that cannot be explained by loss of SHH signaling in the developing forebrain. The cause of these NTDs in $Lrp2^{-/-}$ embryos is so far unknown. NTDs are a group of congenital malformations that occur when the neural tube fails to close during embryonic development. In human pregnancies, NTDs are the second most frequent malformations after congenital heart defects (Wallingford et al., 2013). Among the candidate genes associated with risk for human NTDs are genes important in folate metabolism.

A functional link between LRP2 activity and endocytic folate uptake *in vitro* in kidney sections has been suggested previously (Birn et al., 2005). The binding of soluble folate receptor 1 (sFOLR1; also known as FBP1 or FBP, for folate binding protein) to immobilized LRP2 was shown by surface plasmon resonance analysis, as well as by binding of sFOLR1 to sections of kidney cortex and uptake of sFOLR1 by BN-16 cells. In this study, we addressed the question of whether LRP2 expressed in the developing neural tube is required for the delivery of folate into neuroepithelial cells during neurulation.

RESULTS

Closure of the rostral neural tube is impaired in LRP2-deficient mouse embryos

We systematically examined the neural tube closure phenotype of $Lrp2^{-/-}$ mice and *Shh*-null mutant mice. In agreement with previous reports (Chiang et al., 1996; Murdoch and Copp, 2010), SHH deficiency does not prevent neural tube closure (Fig. 1). Despite impaired specification of the ventral neural tube, 95.5% of all somite-stage 17–26 SHH-deficient embryos showed normal neural tube closure, a number not significantly different from that of wild-type embryos, where rostral neural tube closure is completed at the 15-somite stage [embryonic day (E) 9.0; Fisher's exact test, $P>0.2$] (Fig. 1). By contrast, a significant proportion (38%; Fisher's exact test, $P<0.0001$) of LRP2-deficient embryos exhibited an open rostral neural tube at somite-stages 17–26 (Fig. 1). In all of these cases, the posterior neural tube had closed and, in most of them, the most anterior portion of the forebrain was also closed. This pattern indicates a defect in neural tube closure at the level of Closure 2 (Copp et al., 2003), which is initiated at the forebrain-midbrain boundary, in $Lrp2^{-/-}$ embryos.
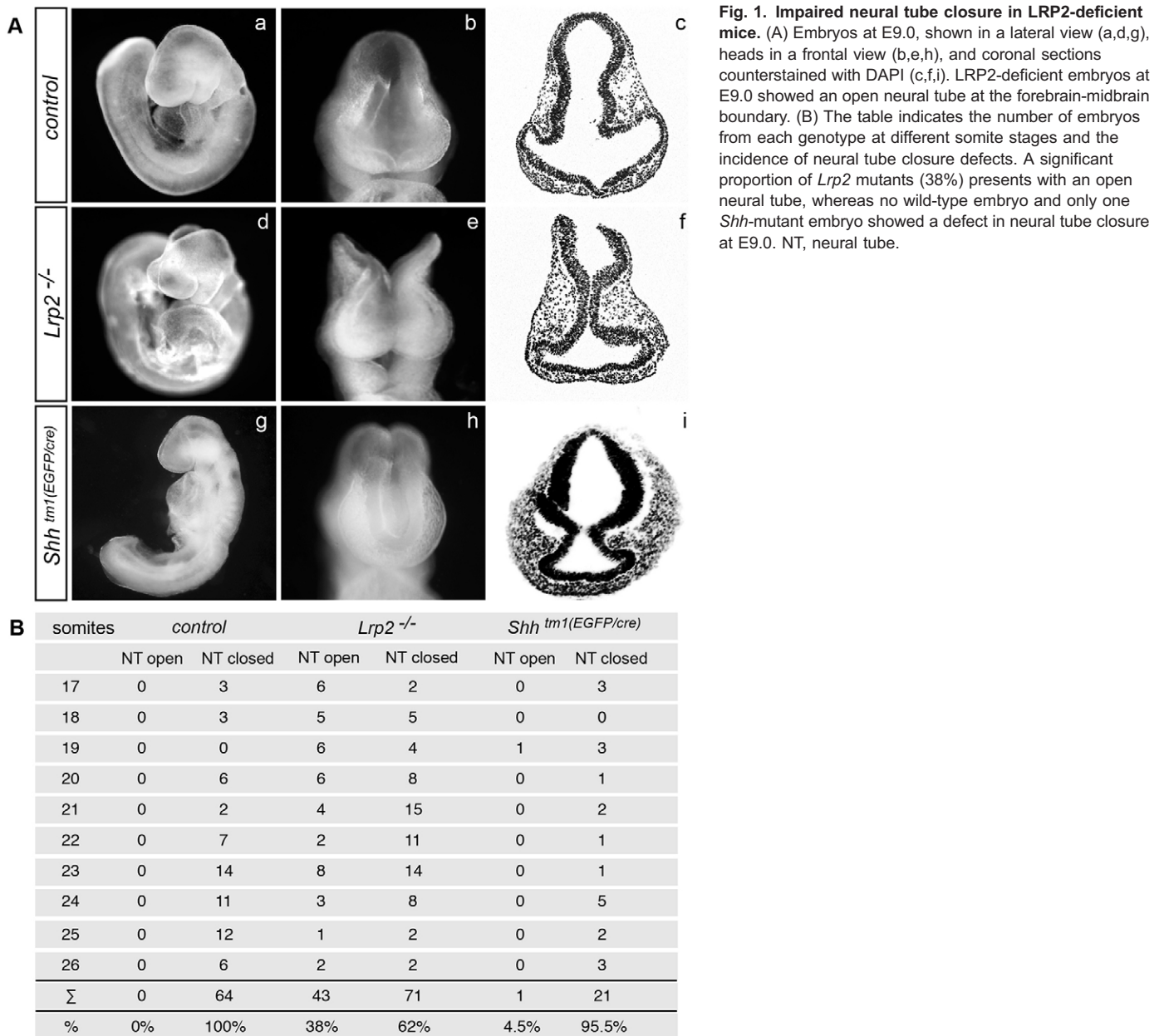
Other LDL receptor family members might be affected in our *Lrp2*-deletion model and might therefore contribute to the NTDs.

[1]Max Delbrück Center for Molecular Medicine (MDC), Robert Rössle Strasse 10, 13125 Berlin, Germany. [2]Department of Nutritional Sciences, Dell Pediatric Research Institute, The University of Texas at Austin, Austin, TX 78723, USA.
*Present address: Department of Neurobiology, Harvard Medical School, Boston, MA 02115, USA.
‡These authors contributed equally to this work

§Author for correspondence (hammes@mdc-berlin.de)

Journal of Cell Science

Fig. 1. Impaired neural tube closure in LRP2-deficient mice. (A) Embryos at E9.0, shown in a lateral view (a,d,g), heads in a frontal view (b,e,h), and coronal sections counterstained with DAPI (c,f,i). LRP2-deficient embryos at E9.0 showed an open neural tube at the forebrain-midbrain boundary. (B) The table indicates the number of embryos from each genotype at different somite stages and the incidence of neural tube closure defects. A significant proportion of *Lrp2* mutants (38%) presents with an open neural tube, whereas no wild-type embryo and only one *Shh*-mutant embryo showed a defect in neural tube closure at E9.0. NT, neural tube.

somites	control		Lrp2 -/-		Shh tm1(EGFP/cre)	
	NT open	NT closed	NT open	NT closed	NT open	NT closed
17	0	3	6	2	0	3
18	0	3	5	5	0	0
19	0	0	6	4	1	3
20	0	6	6	8	0	1
21	0	2	4	15	0	2
22	0	7	2	11	0	1
23	0	14	8	14	0	1
24	0	11	3	8	0	5
25	0	12	1	2	0	2
26	0	6	2	2	0	3
Σ	0	64	43	71	1	21
%	0%	100%	38%	62%	4.5%	95.5%

Loss- and gain-of-function mouse models for LRP6 suffer from compromised neural tube development (Gray et al., 2013; Gray et al., 2010). We thus measured the expression levels of *Lrp1*, *Lrp1b*, *Lrp4*, *Lrp5* and *Lrp6* in the developing brain. As shown in supplementary material Fig. S1, no differences in expression levels of these receptors were detected by comparing mutant with control samples. These results support the idea that the neural tube phenotype is caused by LRP2 deficiency and not by altered expression of other LDL receptor family members.

Endocytosis of FOLR1 and folic acid is impaired in LRP2-deficient mice

One established risk factor for NTDs is impaired uptake of folate (vitamin B$_9$) bound to folate-binding proteins and disturbed metabolism of the vitamin (Gelineau-van Waes et al., 2008a; Piedrahita et al., 1999; Spiegelstein et al., 2004). There are different routes by which cells take up folate. Relevant for

embryonic development of the nervous system are the bidirectional solute carrier family 19 (folate transporter) member 1 (SLC19a1; also known as reduced folate carrier 1, RFC1) and the folate receptor 1 (FOLR1; also known as folate binding protein, FBP1), which exists both as a glycosylphosphatidylinositol (GPI)-anchored and as a soluble isoform, sFOLR1 (Lacey et al., 1989; Spiegelstein et al., 2000). FOLR1 regulates folate uptake through endocytic mechanisms and is important for proper neural tube closure (Piedrahita et al., 1999; Tang and Finnell, 2003). Because none of the FOLR1 receptor isoforms contains a transmembrane segment, high efficiency uptake relies on their association with an additional as-yet-unidentified transmembrane receptor.

We asked whether LRP2 might mediate the uptake of FOLR1 *in vivo*. To test this hypothesis, we injected adult control and LRP2-deficient mice with Alexa-Fluor-488 (A488)-labeled sFOLR1. After 2 hours, the labeled protein was detectable in

intracellular compartments of kidney proximal tubules of control mice (Fig. 2A). By contrast, no uptake was seen in LRP2-deficient animals (Fig. 2A), indicating that LRP2 is required for efficient uptake of sFOLR1 *in vivo*.

We next tested whether LRP2 is required for cellular uptake of sFOLR1 in neuroepithelial cells during neurulation stages. To this end, we cultured control and LRP2-deficient E8.5 embryos before neural tube closure in medium containing A488-labeled sFOLR1. After 2 hours of incubation, sFOLR1 could be detected bound to the surface and within the apical compartment of control neuroepithelial cells (Fig. 2B). However, no sFOLR1 was detectable in the LRP2-deficient neuroepithelium (Fig. 2B).
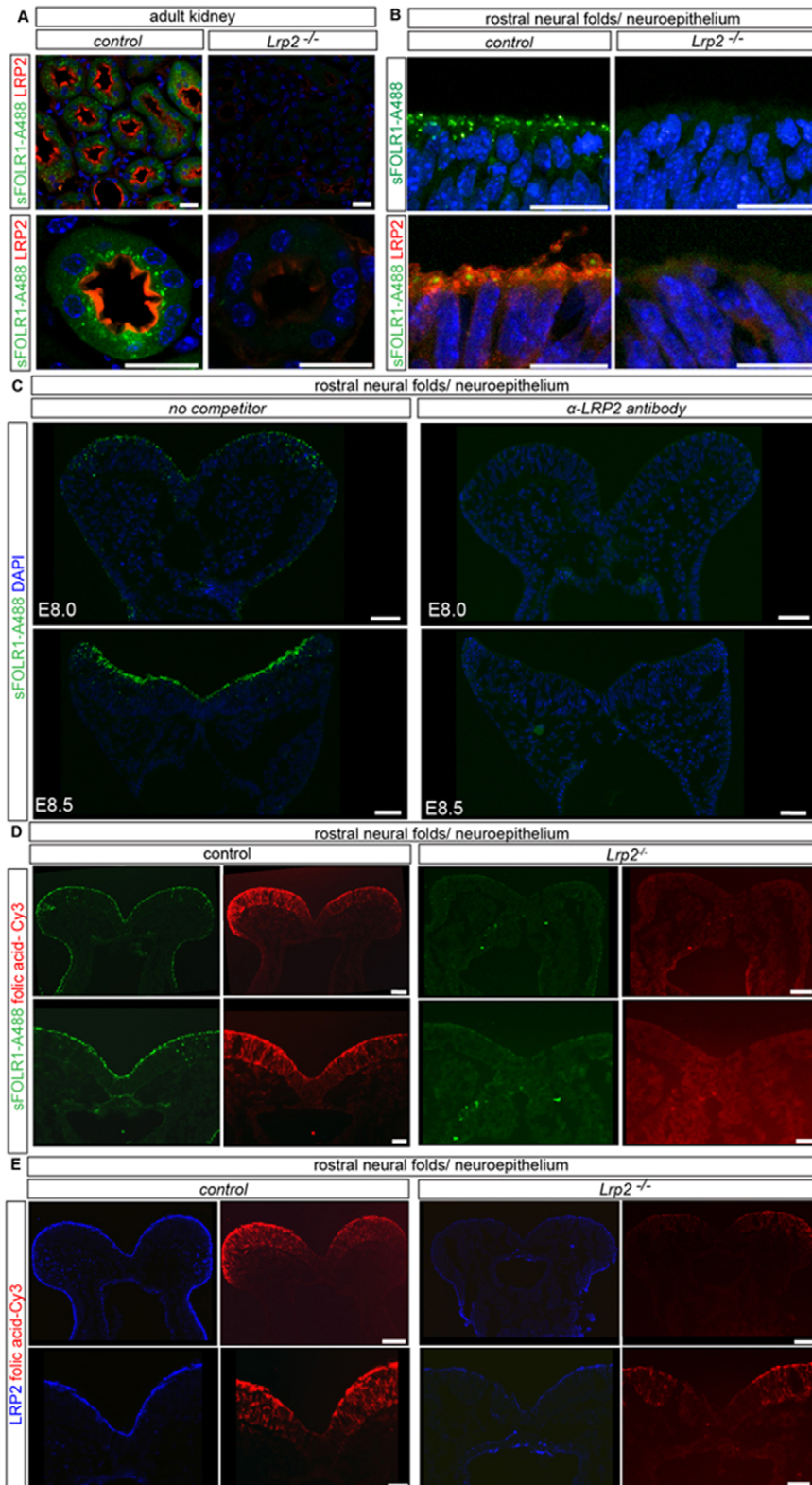
Fig. 2. Uptake studies for sFOLR1 and folic acid in whole-embryo cultures. (A) Immunohistological detection of LRP2 (red) and sFOLR1–A488 (green) on kidney sections from adult *Lrp2* mutants (*n*=2) and wild-type controls (*n*=2) injected with sFOLR1–A488. The absence of LRP2 in mutant mice results in impaired binding to and uptake of sFOLR1 at the apical surface of kidney proximal tubule cells. Scale bars: 20 µm. (B) Immunohistological detection of LRP2 (red) and sFOLR1–A488 (green) on coronal sections from E8.5 whole-embryo cultures incubated with sFOLR1–A488. No sFOLR1–A488 signal was seen in *Lrp2*-mutant embryonic neural folds (*n*=6), compared with a robust signal in control littermates (*n*=27). The pictures show neuroepithelial tissue from coronal sections of rostral neural folds. Scale bars: 20 µm. (C) Adding anti-LRP2 antibody as a competitor in sFOLR1-uptake studies completely blocked internalization of sFOLR1–A488 in neuroepithelial tissue from control embryos (*n*=5), whereas neuroepithelial tissue without competitor showed uptake of sFOLR1–A488 (*n*=5). The pictures show coronal sections of rostral neural folds before closure at E8.0 and E8.5. Scale bars: 50 µm. Nuclei are stained with DAPI (blue) in A–C. (D) Immunohistological detection of sFOLR1–A488 (green) and folic-acid–Cy3 (red) on coronal sections of E8.5 whole-embryo cultures incubated with folic-acid–Cy3 and sFOLR1–A488. Robust uptake was seen in wild-type samples (*n*=12) compared with *Lrp2*^{−/−} rostral neural folds (*n*=3), which showed no detectable signals for sFOLR1–A488 and very weak signals for folic-acid–Cy3. For each genotype, higher magnification of the rostral neural folds are shown in the lower panels. Scale bars: 50 µm (upper panels), 25 µm (lower panels). (E) Immunohistological detection of LRP2 (blue) and folic-acid–Cy3 (red) on coronal sections of E8.5 whole-embryo cultures incubated with folic-acid–Cy3. Robust uptake was seen in wild-type rostral neural folds (*n*=7) compared with *Lrp2*^{−/−} neural folds (*n*=4), which showed only weak signals for folic-acid–Cy3. Lower panels show higher magnification of the coronal section of the neural folds. Scale bars: 50 µm (upper panels), 25 µm (lower panels).

Furthermore, adding inhibitory anti-LRP2 antibody blocked sFOLR1 uptake in wild-type neuroepithelial cells (Fig. 2C). These results indicate that LRP2, expressed in the neuroepithelium, is required for the cellular uptake of sFOLR1 during neurulation. To exclude the possibility that LRP2 facilitates endocytosis of the A488 tag we incubated wild-type embryos with sFOLR1–Alexa-Fluor-647 (A647) and GST–A488. No uptake of GST–A488 was seen in these experiments, whereas uptake was seen for sFOLR1–A647 (supplementary material Fig. S2).

We next examined whether LRP2-mediated uptake of FOLR1 results in the simultaneous uptake of folic acid bound to this carrier. To do so, whole-embryo cultures were incubated with Cy3-labeled folic acid complexed with sFOLR1–A488. Uptake experiments showed intracellular signals both for sFOLR1–A488 and Cy3-labeled folic acid in the neuroepithelial tissue of E8.5 wild-type mouse embryos. However, no sFOLR1–A488 uptake, and severely reduced internalization of folic-acid–Cy3, was observed in the rostral neural folds of $Lrp2^{-/-}$ littermates (Fig. 2D). Thus, LRP2 appears to present the main uptake pathway for this vitamin in the neural tube. To explore sFOLR1-independent uptake of folic acid, we incubated embryo cultures with folic-acid–Cy3 without adding soluble FOLR1, under serum-free conditions. In this scenario, the GPI-anchored FOLR1 should be able to mediate vitamin uptake both in wild-type and mutant embryos. However, also in this case, LRP2-deficient neural folds showed reduced uptake of folic acid compared with wild-type tissue (Fig. 2E), indicating that internalization of the complex formed by folic acid and GPI−FOLR1 is also dependent on LRP2 (see model, Fig. 5).

Taken together, these experiments demonstrate that efficient cellular uptake of folic acid and its binding proteins sFOLR1 and GPI–FOLR1 is mediated in a LRP2-dependent manner at the apical surface of the developing neuroepithelium. Importantly, our results suggest that endocytosis of a vitamin-binding protein, in this case FOLR1, by LRP2 directly influences crucial events during embryonic development, as cellular uptake of folate is required for the normal progression of neural tube closure.

Decreased folate concentrations in $Lrp2^{-/-}$ embryos
To investigate whether the impaired uptake of FOLR1 caused by LRP2 deficiency in the neuroepithelium influences folate concentrations in the embryonic neuroepithelium, we determined tissue folate levels in E9.5 $Lrp2^{-/-}$ embryos and somite-matched control littermates. Folate concentrations were significantly lower in tissue samples isolated from LRP2-deficient embryonic anterior neural tube compared with samples derived from control embryos (Fig. 3A). This finding is consistent with an impaired uptake of folic acid and FOLR1 in the neuroepithelium of LRP2-deficient embryos.

FOLR1 and LRP2 have overlapping expression domains in the developing neural tube
To provide further evidence for a functional link between FOLR1 and LRP2, we carefully compared the expression pattern and protein localization in the developing brain of E9.5 and E10.5 embryos (supplementary material Fig. S3). The most prominent overlap for LRP2 and FOLR1 was seen in the dorsal neuroepithelial midline, which corresponds to the site where Closure 2 is initiated, and in the ventral midline of the midbrain neuroepithelium.

Folr1 and Slc19a1 expression in $Lrp2^{-/-}$ mutants
We next asked whether the impaired uptake of folate and decreased tissue folate concentrations are primary consequences

of LRP2 deficiency rather than of defects in the expression of folate receptors and carriers. We thus examined the expression of FOLR1 (protein and mRNA) and *Slc19a1* (mRNA) in *Lrp2* mutants and in control littermates. Using *in situ* hybridization and immunohistochemistry, we showed that the expression pattern of FOLR1 in the neural tube of LRP2-deficient embryos was comparable to that of wild-type controls (Fig. 3B). The expression levels of *Folr1* and *Slc19a1* were significantly increased in $Lrp2^{-/-}$ embryonic heads compared with their expression in control samples (Fig. 3C,D), a fact that could be explained by a compensatory upregulation of folate receptors and folate carriers in response to LRP2 deficiency.

In the kidney, where LRP2 mediates the uptake of sFOLR1 into proximal tubule cells (Fig. 2A), the expression pattern of *Folr1* mRNA and the immunohistological detection of FOLR1 protein was not different between $Lrp2^{-/-}$ and control kidneys (Fig. 3E,F). Thus, a loss of expression of the established folate receptors or carriers does not account for the defects in folate metabolism seen in LRP2-deficient organisms.

Expression of the folate-dependent gene *Alx3* is reduced in LRP2-deficient embryos
Little is known about the mechanisms underlying the rescue of neural tube closure defects by folate. Recently, it was shown that expression of the gene *Alx3* (aristaless-family homeobox transcription factor 3) is specifically dependent on folate, and that ALX3 is important for neural tube closure (Kessaris et al., 2006; Lakhwani et al., 2010).

In situ hybridization analysis and quantitative RT-PCR showed that *Alx3* mRNA expression was reduced in LRP2-deficient embryos compared with controls (Fig. 4A,C). Interestingly, expression of the *Alx3*-related folate-independent transcription factor *Alx4* (Lakhwani et al., 2010) was unchanged in LRP2-deficient embryos (Fig. 4B,C). Importantly, impaired *Alx3* expression in LRP2-deficient embryos is unlikely to be a downstream effect of aberrant SHH signaling, because we detected normal expression patterns and mRNA levels of *Alx3* in *Shh*-mutant embryos (Fig. 4A,C). These findings suggest that in the absence of LRP2, the endocytosis of folate is impaired, leading to alterations in the expression of folate-dependent genes including *Alx3*, ultimately contributing to the pathogenesis of NTDs.

DISCUSSION
Over the past years it became well accepted that members of the LDL receptor family, including LRP2, play an important role in signaling during embryonic development. Here, we show that LRP2 is essential for the uptake of folic acid and folate receptors in the developing neural tube. Our results also demonstrate that LRP2 deficiency leads to impaired cellular uptake of folate during neurulation and impaired expression of the transcription factor *Alx3*, which likely contributes to rostral neural tube closure defects in $Lrp2^{-/-}$ embryos.

LRP2 is a multifunctional endocytic receptor expressed early in embryonic development on the apical surface of the neuroepithelium. In our recent work, we established a role for LRP2 in the ventral midline of the rostral diencephalon, where the receptor mediates SHH signal transduction in the early embryo, acting as a co-receptor for patched1 (Christ et al., 2012). However, the function of LRP2 in other neural tube domains during embryonic development remained unclear. Here, we postulate that LRP2 plays a role in the process of neural tube
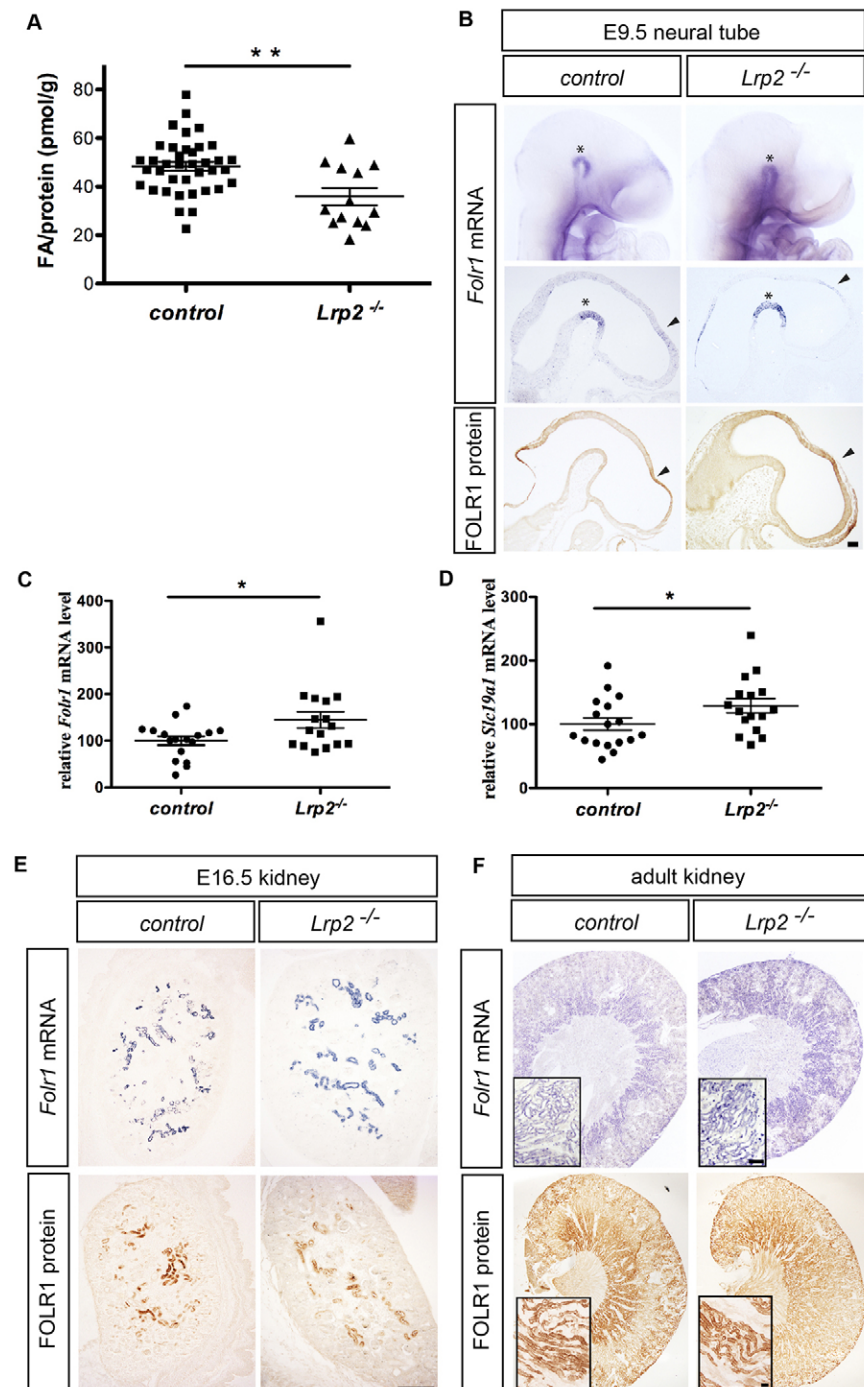
Fig. 3. Reduced tissue folate concentrations in _Lrp2_^{−/−} embryos are not caused by impaired _Folr1_ or _Slc19a1_ expression. (A) Cranial tissue folate (FA) concentrations in E9.5 _Lrp2_$^{-/-}$ embryos were significantly lower compared with samples derived from somite-matched control embryos. Wild-type and heterozygous littermates were pooled because they showed identical phenotypes. _Lrp2_$^{-/-}$, $n=13$; _Lrp2_$^{+/+}$, $n=17$; _Lrp2_$^{+/-}$, $n=21$. The mean±s.e.m. is indicated; **$P=0.0017$. (B) _In situ_ hybridization analyses on whole-mount E9.5 embryos (upper panel) and on sagittal E9.5 brain paraffin sections (middle and lower panels) demonstrate the expression pattern for _Folr1_ in the ventral neural tube (asterisk) and in the dorsal forebrain (arrowhead), which shows no difference between _Lrp2_$^{-/-}$ embryos ($n=10$) and somite-matched controls ($n=12$). Immunohistological detection of FOLR1 on sagittal E9.5 brain paraffin sections confirmed the expression pattern data seen in ISH experiments (see also supplementary material Fig. S3). Scale bar: 50 µm. (C,D) Quantitative RT-PCR analyses on head mRNA samples from E9.5 embryos (21–24 somites) revealed significantly higher expression levels of _Folr1_ and _Slc19a1_ in _Lrp2_ mutants compared with wild-type controls. _Lrp2_$^{+/+}$, $n=17$; _Lrp2_$^{-/-}$, $n=16$. The mean±s.e.m. is indicated; *$P=0.0254$ (C), *$P=0.0385$ (D). (E,F) In E16.5 and adult kidneys from _Lrp2_$^{-/-}$ mice, _Folr1_ mRNA is correctly expressed as demonstrated in ISH experiments. The protein is localized on the apical surface of proximal tubule cells in LRP2-deficient mice, comparable to controls, as shown in immunohistological analyses on sagittal kidney sections (10 µm paraffin sections). Scale bars: 100 µm.

closure, because 38% of LRP2-deficient embryos showed impaired rostral neural tube closure, which is unlikely to be linked to loss of SHH signals (Fig. 1) (Chiang et al., 1996; Murdoch and Copp, 2010).

Folic acid (vitamin B₉) is known to reduce the risk of human NTDs, and mouse models with loss-of-function mutations affecting the _Folr1_ or _Slc19a1_ genes show NTDs and embryonic lethality (Blom et al., 2006; Cabrera et al., 2004; Gelineau-van Waes et al., 2008a; Piedrahita et al., 1999; Zhao et al., 2001). LRP2 has been shown to mediate the uptake of many hormones and vitamins bound to their respective carrier proteins, including vitamin D-binding protein (DBP), retinol-binding protein (RBP)

and sex hormone-binding globulins (SHBG). Impaired uptake of these complexes in LRP2-deficient mice affects adult vitamin homeostasis (DBP and RBP) as well as late embryonic and early postnatal development (SHBG) (Christensen et al., 1999; Hammes et al., 2005; Nykjaer et al., 1999).

A functional link between LRP2 activity in the kidney and endocytic uptake of folic acid and the folate receptor has been suggested (Birn et al., 2005). Additional evidence for the role of LRP2 in folate uptake in embryonic tissue comes from a study by Gelineau-van-Waes and colleagues, showing that components of the LRP2–cubilin receptor complex are upregulated in SLC19a1-deficient embryos (Gelineau-van Waes et al., 2008b). Thus,
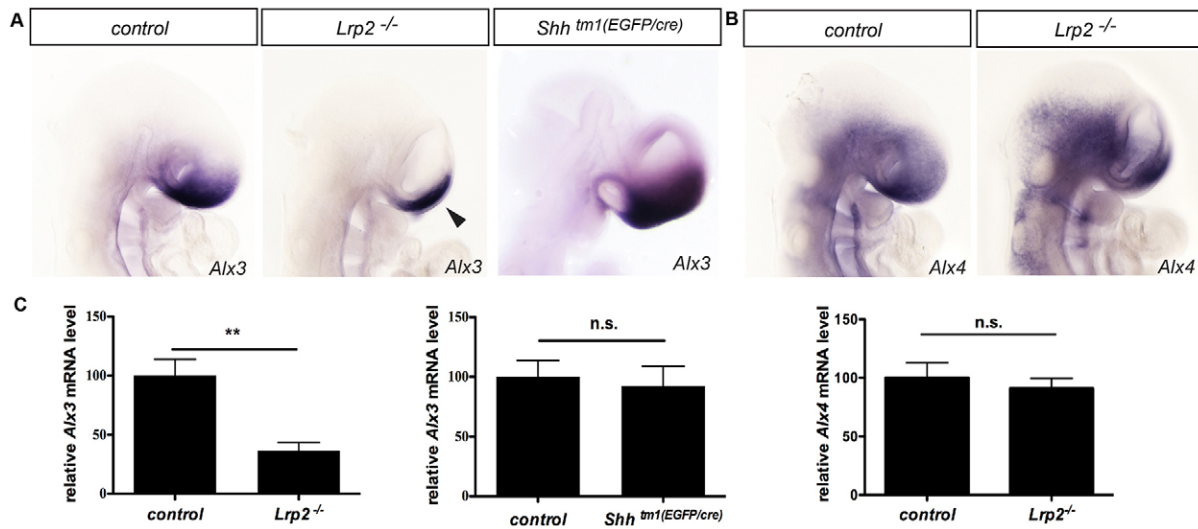
Fig. 4. Reduced *Alx3* expression in LRP2-deficient embryos. (A) Whole-mount *in situ* hybridization analyses demonstrate reduced *Alx3* expression in the rostral forebrain of *Lrp2*$^{-/-}$ embryos at E9.5 (arrowhead) compared with wild-type controls and *Shh*$^{tm1(EGFP/cre)}$ mutant embryos. *Lrp2*$^{+/+}$, n=5; *Lrp2*$^{-/-}$, n=4; *Shh*$^{+/+}$, n=4; *Shh*$^{-/-}$, n=4. (B) The expression pattern of *Alx4* is unchanged in the neural tube of *Lrp2*$^{-/-}$ embryos at E9.5 compared with that of controls, as shown by whole-mount *in situ* hybridization. n=3 for both genotypes. (C) Quantitative RT-PCR analyses on embryonic head samples at somite-stages 21–24 from *Lrp2*$^{-/-}$ mutants, *Shh*$^{tm1(EGFP/cre)}$ mutants and controls confirmed that there were significantly reduced levels of *Alx3* expression in LRP2-deficient embryonic heads compared with those of littermate controls. *Lrp2*$^{+/+}$, n=2; *Lrp2*$^{+/-}$, n=3; *Lrp2*$^{-/-}$, n=5. **P=0.0031. By contrast, *Shh*-null mutants showed no significant difference in *Alx3* expression levels compared with those of controls. *Shh*$^{+/+}$, n=5; *Shh*$^{+/-}$, n=2; *Shh*$^{-/-}$, n=6. P=0.7261. No difference in *Alx4* expression levels was seen between *Lrp2*-mutant and control samples. *Lrp2*$^{+/+}$, n=12; *Lrp2*$^{-/-}$, n=11. P=0.9558. Wild-type and heterozygous littermates were pooled in these experiments because they showed identical phenotypes. Data are shown as the mean±s.e.m.; n.s., non-significant.

increased expression of *Lrp2* could compensate for the lack of folate uptake through SLC19a1 by increasing the folate uptake through FOLR1 and LRP2. Our results demonstrate that LRP2 plays an essential role in the uptake of folic acid and its binding protein FOLR1 in the developing neural tube (Fig. 2). LRP2 deficiency leads to impaired cellular uptake of folate during neurulation, which might consequently contribute to NTDs in *Lrp2*$^{-/-}$ embryos.
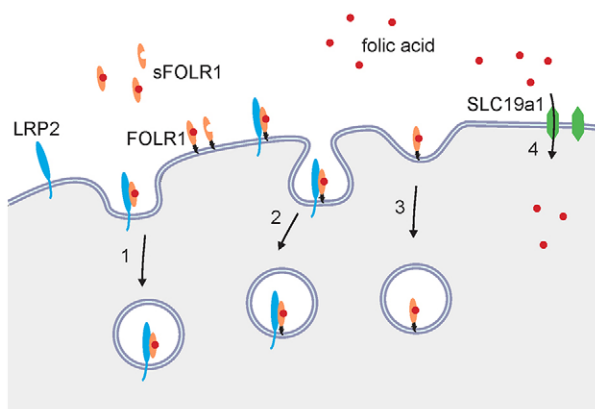

Fig. 5. Model depicting the possible routes of folic acid uptake into neuroepithelial cells. Soluble FOLR1 (sFOLR1) and GPI-anchored FOLR1 bind to folic acid, and the uptake of the complex is mediated through endocytic mechanisms. High-efficiency internalization of sFOLR1 and GPI–FOLR1 relies on their interaction with a co-receptor spanning the plasma membrane, which, according to our results, is likely to be LRP2 (route 1 and 2). Less-efficient uptake is probably mediated by alternative routes (3), which are not yet well understood (Mayor and Riezman, 2004). Carrier-mediated uptake of folic acid (4) occurs through SLC19a1.

The weak uptake of folic acid seen in *Lrp2*$^{-/-}$ tissue (as shown in Fig. 2D,E) might be explained by the internalization of folic acid through LRP2-independent routes. For example, folic acid can enter the cell by the folate carrier SLC19a1. Expression levels for this folate carrier are upregulated in LRP2-deficient embryos (Fig. 3C,D), indicating a compensatory effect as a consequence of impaired LRP2- and FOLR1-mediated uptake of folate. However, considering the weak uptake of folic acid in LRP2-deficient tissue, the SLC19a1-mediated folic acid uptake and alternative routes for the uptake of sFOLR1 or GPI–FOLR1 (depicted in Fig. 5) seem to play a minor role in the efficient uptake of folic acid in the neural folds. This further supports the hypothesis that efficient uptake of folate is dependent on co-receptor-mediated endocytosis of sFOLR1 and GPI–FOLR1.

A putative co-receptor for FOLR1 had not yet been identified. Our data suggest that the endocytosis of soluble FOLR1 and membrane-anchored GPI–FOLR1 requires the interaction of these proteins with the single-spanning transmembrane endocytic receptor LRP2 (Fig. 5). This 'dual-receptor complex' hypothesis for the uptake of folate is analogous to the uptake of renal and intestinal vitamin B$_{12}$ bound to intrinsic factor through cubilin, a peripherally attached glycoprotein. Internalization of the cubilin–ligand complex strongly relies on the interaction with LRP2 (Denz-Penhey and Murdoch, 2009; Horbinski et al., 2009).

Gene defects and environmental factors, or a combination thereof, can cause NTDs. Studies on animal models have identified a large number of candidate genes involved in the etiology of NTDs (Harris and Juriloff, 2010). In humans, however, little is known about the interaction of most of these risk genes and the maternal factors. Therefore, further experiments will be required to elucidate the mechanisms underlying the protective effects of maternal folic acid supplementation for the embryo (Blom et al., 2006; Finnell

et al., 2010; Wallingford et al., 2013). Moreover, to better understand the molecular mechanisms of LRP2-dependent NTDs, it remains to be investigated whether other factors, such as altered morphogen pathways, cilia function and apico-basal polarity of neuroepithelial cells (Eom et al., 2011), function in addition to the impaired folate uptake to modulate the NTD phenotype in LRP2-deficient mice.

MATERIALS AND METHODS
Mouse models
The generation of mice with targeted disruption of the *Lrp2* gene has been described previously (Willnow et al., 1996). Analyses of the embryonic neural tube defects were carried out in LRP2-deficient and in somite-matched wild-type and heterozygous littermates on a C57BL/6N background. Wild-type and heterozygous littermates show no differences in any of the analyses, and both genotypes are therefore referred to as controls in the experiments. sFOLR1-uptake studies in the kidney were performed on LRP2-deficient mice on an inbred FVB/N genetic background, because surviving adult LRP2-deficient mice can be obtained on this genetic background. *Shh*[tm1(EGFP/cre)] mutant mice (Harfe et al., 2004), kindly provided by Clifford Tabin (Harvard Medical School, Boston, MA) were used to analyze the neural tube phenotype in SHH-deficient embryos and wild-type somite-matched littermates. All experiments involving animals were performed according to institutional guidelines following approval by local authorities.

Uptake studies
sFOLR1–A488, sFOLR1–A647 and GST–A488 were generated by labeling folate-binding protein from bovine milk (F0504, Sigma) and GST using the Alexa Fluor 488 or Alexa Fluor 647 protein labeling kit (A10235, A20173, Life Technologies). Cy3–PEG-folic acid was obtained from Nanocs (PG2-FAS3-3k). E8.0 and E8.5 embryos were incubated in their yolk sacs in DMEM containing 5 µg/ml sFOLR1–A488, sFOLR1–A647, GST–A488 or folic-acid–Cy3 at 37℃ under 5% CO_2 and 95% humidity. Folic-acid–Cy3 was incubated with sFOLR1–A488 for 30 minutes at room temperature before adding both reagents to the embryo culture. The yolk sac and amnion were opened by an incision to enable the diffusion of proteins. After 2 hours of incubation, the yolk sac and amnion were removed, and embryos were fixed in 4% paraformaldehyde (PFA) for 15 minutes. Embryos were cryosectioned at 10 µm. LRP2 receptor activity was blocked by incubation with goat anti-LRP2 antiserum (1:100); controls received goat non-immune serum (1:100).

To test sFOLR1 uptake by kidney proximal tubule cells, sFOLR1–A488 was injected into the tail veins of adult mice (300 ng/µl in PBS; 180 µl total volume). After 90 minutes, animals were sacrificed and kidneys were isolated and fixed in 4% PFA (at room temperature for 90 minutes). Kidneys were cryosectioned at 12 µm.

Measurement of reduced folate concentrations in mouse embryonic tissue
Folate to total protein ratios (nmole/g) were determined for head tissue samples from LRP2-deficient embryos ($n=13$; 23–26 somites) and somite-matched heterozygous ($n=21$) and wild-type ($n=17$) controls. The assay procedure used to identify the concentration of folate in tissue samples was a modification of the folate-inhibition assay (Cabrera et al., 2008). Briefly, 50 µg/ml bovine folate-binding protein (Sigma Aldrich, St Louis, MO), diluted in 100 mM NaHCO3 pH 8.3, was printed onto the plate surface in 2 µl volumes at 4℃ overnight. Sample tissues were suspended in 150 µl of lysis buffer [1× PBS, 0.1% Tween (v/v), 1% ascorbate (w/v)]. Samples were homogenized mechanically and placed in a boiling water bath for 10 minutes. Samples were then spun at 14,000 g for 7 minutes, and the supernatant was collected. A volume of 2 µl of 5% NaOH (w/v) was added for neutralization of the solution. Unlabeled folic acid was spiked by serial dilution (250–0.244 ng/ml) in PBS-Tween buffer in order to generate a standard regression curve for the determination of relative folate concentrations in samples. Standard and sample solutions were mixed 1:5 with horseradish peroxidase (HRP)-labeled folic acid solution (FA–HRP; Ortho-Clinical Diagnostics, Raritan, NJ) and incubated in sample wells for 2 hours. Plates were washed six times with 1× PBS-Tween, and the HRP signal was detected with SuperSignal ELISA Femto Substrate (Pierce). The 96-well plates were imaged and analyzed on a Q-view chemiluminescent imager (Quansys Biosciences). Data were analyzed in GraphPad Prism (GraphPad Software) using a Student's *t*-test.

Immunohistological analysis
Standard immunohistochemical analysis was performed by incubation of tissue sections with the following primary antibodies at the indicated dilutions; sheep anti-LRP2 antiserum (1:5000; kindly provided by Renata Kozyraki, Institute De La Vision, Paris) and rabbit anti-FOLR1 (1:500; Abcam). Bound primary antibodies were visualized using secondary antisera conjugated with Alexa Fluor 488, 555 or 647 (1:500; Invitrogen). Nuclei were counterstained with DAPI (1:8000; Roche). Alternatively, bound primary antibodies were visualized with secondary antisera conjugated with biotin (1:300), avidin–biotin complex (ABC; 1:300; Vectastain) or diaminobenzidine (DAB; Sigma Aldrich). Analyses were performed using a Leica SPE confocal microscope and Leica DMI6000B.

In situ hybridization
Whole-mount *in situ* hybridization (WISH) was performed as described previously (Hammes et al., 2001). *In situ* hybridization (ISH) on sections was performed as described previously (Travers and Haas, 2004). Plasmids were purchased from Source Bioscience: *FolR1*, IRAKp961N1711Q; *Alx3*, D230004L08; *Alx4*, IRAVp968G0971D.

Quantitative RT-PCR
Total RNA from E9.5 embryo heads was extracted using an RNeasy Micro kit (Qiagen). cDNA was synthesized by using the High Capacity RNA-to-cDNA kit (Life technologies), and quantitative PCR was performed using an ABI7900. The expression of *Alx3*, *FolR1* and *Slc19a1* was normalized to that of *Gapdh* (Mm99999915_g1; Life Technologies). The following gene expression assays were used: *Alx3*, Mm01204737_m1; *Alx4*, Mm00431780_m1; *Folr1*, Mm00433355_m1; *Slc19a1*, Mm00446220_m1; *Lrp1*, Mm00464608_m1; *Lrp1b*, Mm00466712_m1; *Lrp4*, Mm00554326_m1; *Lrp5*, Mm01227476_m1; and *Lrp6*, Mm00999795_m1 (Life Technologies). Data were analyzed in GraphPad Prism (GraphPad Software) using an unpaired Student's *t*-test.

Author contributions
E.K. and A.H. developed the concept; E.K. and N.M. designed and performed experiments and analyzed the data; R.M.C. carried out experiments and analyzed the data; T.E.W. analyzed data; A.H. designed the experiments, analyzed data and wrote the manuscript with contributions from all the authors.

Supplementary material
Supplementary material available online at
http://jcs.biologists.org/lookup/suppl/doi:10.1242/jcs.140145/-/DC1

References
Birn, H., Zhai, X., Holm, J., Hansen, S. I., Jacobsen, C., Christensen, E. I. and Moestrup, S. K. (2005). Megalin binds and mediates cellular internalization of folate binding protein. *FEBS J.* **272**, 4423-4430.

Blom, H. J., Shaw, G. M., den Heijer, M. and Finnell, R. H. (2006). Neural tube defects and folate: case far from closed. *Nat. Rev. Neurosci.* **7**, 724-731.

Cabrera, R. M., Hill, D. S., Etheredge, A. J. and Finnell, R. H. (2004). Investigations into the etiology of neural tube defects. *Birth Defects Res. C Embryo Today* **72**, 330-344.

Cabrera, R. M., Shaw, G. M., Ballard, J. L., Carmichael, S. L., Yang, W., Lammer, E. J. and Finnell, R. H. (2008). Autoantibodies to folate receptor during pregnancy and neural tube defect risk. *J. Reprod. Immunol.* **79**, 85-92.

Chiang, C., Litingtung, Y., Lee, E., Young, K. E., Corden, J. L., Westphal, H. and Beachy, P. A. (1996). Cyclopia and defective axial patterning in mice lacking Sonic hedgehog gene function. *Nature* **383**, 407-413.

Christ, A., Christa, A., Kur, E., Lioubinski, O., Bachmann, S., Willnow, T. E. and Hammes, A. (2012). LRP2 is an auxiliary SHH receptor required to condition the forebrain ventral midline for inductive signals. *Dev. Cell* **22**, 268-278.

Christensen, E. I., Moskaug, J. O., Vorum, H., Jacobsen, C., Gundersen, T. E., Nykjaer, A., Blomhoff, R., Willnow, T. E. and Moestrup, S. K. (1999). Evidence for an essential role of megalin in transepithelial transport of retinol. *J. Am. Soc. Nephrol.* **10**, 685-695.

Copp, A. J., Greene, N. D. and Murdoch, J. N. (2003). The genetic basis of mammalian neurulation. *Nat. Rev. Genet.* **4**, 784-793.

Denz-Penhey, H. and Murdoch, J. C. (2009). A comparison between findings from the DREEM questionnaire and that from qualitative interviews. *Med. Teach.* **31**, e449-e453.

Eom, D. S., Amarnath, S., Fogel, J. L. and Agarwala, S. (2011). Bone morphogenetic proteins regulate neural tube closure by interacting with the apicobasal polarity pathway. *Development* **138**, 3179-3188.

Finnell, R. H., Blom, H. J. and Shaw, G. M. (2010). Does global hypomethylation contribute to susceptibility to neural tube defects? *Am. J. Clin. Nutr.* **91**, 1153-1154.

Gelineau-van Waes, J., Heller, S., Bauer, L. K., Wilberding, J., Maddox, J. R., Aleman, F., Rosenquist, T. H. and Finnell, R. H. (2008a). Embryonic development in the reduced folate carrier knockout mouse is modulated by maternal folate supplementation. *Birth Defects Res. A Clin. Mol. Teratol.* **82**, 494-507.

Gelineau-van Waes, J., Maddox, J. R., Smith, L. M., van Waes, M., Wilberding, J., Eudy, J. D., Bauer, L. K. and Finnell, R. H. (2008b). Microarray analysis of E9.5 reduced folate carrier (RFC1; Slc19a1) knockout embryos reveals altered expression of genes in the cubilin-megalin multiligand endocytic receptor complex. *BMC Genomics* **9**, 156.

Gray, J. D., Nakouzi, G., Slowinska-Castaldo, B., Dazard, J. E., Rao, J. S., Nadeau, J. H. and Ross, M. E. (2010). Functional interactions between the LRP6 WNT co-receptor and folate supplementation. *Hum. Mol. Genet.* **19**, 4560-4572.

Gray, J. D., Kholmanskikh, S., Castaldo, B. S., Hansler, A., Chung, H., Klotz, B., Singh, S., Brown, A. M. and Ross, M. E. (2013). LRP6 exerts non-canonical effects on Wnt signaling during neural tube closure. *Hum. Mol. Genet.* **22**, 4267-4281.

Hammes, A., Guo, J. K., Lutsch, G., Leheste, J. R., Landrock, D., Ziegler, U., Gubler, M. C. and Schedl, A. (2001). Two splice variants of the Wilms' tumor 1 gene have distinct functions during sex determination and nephron formation. *Cell* **106**, 319-329.

Hammes, A., Andreassen, T. K., Spoelgen, R., Raila, J., Hubner, N., Schulz, H., Metzger, J., Schweigert, F. J., Luppa, P. B., Nykjaer, A. et al. (2005). Role of endocytosis in cellular uptake of sex steroids. *Cell* **122**, 751-762.

Harfe, B. D., Scherz, P. J., Nissim, S., Tian, H., McMahon, A. P. and Tabin, C. J. (2004). Evidence for an expansion-based temporal Shh gradient in specifying vertebrate digit identities. *Cell* **118**, 517-528.

Harris, M. J. and Juriloff, D. M. (2010). An update to the list of mouse mutants with neural tube closure defects and advances toward a complete genetic perspective of neural tube closure. *Birth Defects Res. A Clin. Mol. Teratol.* **88**, 653-669.

Horbinski, C., Kofler, J., Kelly, L. M., Murdoch, G. H. and Nikiforova, M. N. (2009). Diagnostic use of IDH1/2 mutation analysis in routine clinical testing of formalin-fixed, paraffin-embedded glioma tissues. *J. Neuropathol. Exp. Neurol.* **68**, 1319-1325.

Kantarci, S., Al-Gazali, L., Hill, R. S., Donnai, D., Black, G. C., Bieth, E., Chassaing, N., Lacombe, D., Devriendt, K., Teebi, A. et al. (2007). Mutations in LRP2, which encodes the multiligand receptor megalin, cause Donnai-Barrow and facio-oculo-acoustico-renal syndromes. *Nat. Genet.* **39**, 957-959.

Kessaris, N., Fogarty, M., Iannarelli, P., Grist, M., Wegner, M. and Richardson, W. D. (2006). Competing waves of oligodendrocytes in the forebrain and postnatal elimination of an embryonic lineage. *Nat. Neurosci.* **9**, 173-179.

Lacey, S. W., Sanders, J. M., Rothberg, K. G., Anderson, R. G. and Kamen, B. A. (1989). Complementary DNA for the folate binding protein correctly predicts anchoring to the membrane by glycosyl-phosphatidylinositol. *J. Clin. Invest.* **84**, 715-720.

Lakhwani, S., García-Sanz, P. and Vallejo, M. (2010). Alx3-deficient mice exhibit folic acid-resistant craniofacial midline and neural tube closure defects. *Dev. Biol.* **344**, 869-880.

Mayor, S. and Riezman, H. (2004). Sorting GPI-anchored proteins. *Nat. Rev. Mol. Cell Biol.* **5**, 110-120.

Murdoch, J. N. and Copp, A. J. (2010). The relationship between sonic Hedgehog signaling, cilia, and neural tube defects. *Birth Defects Res. A Clin. Mol. Teratol.* **88**, 633-652.

Nykjaer, A. and Willnow, T. E. (2002). The low-density lipoprotein receptor gene family: a cellular Swiss army knife? *Trends Cell Biol.* **12**, 273-280.

Nykjaer, A., Dragun, D., Walther, D., Vorum, H., Jacobsen, C., Herz, J., Melsen, F., Christensen, E. I. and Willnow, T. E. (1999). An endocytic pathway essential for renal uptake and activation of the steroid 25-(OH) vitamin D3. *Cell* **96**, 507-515.

Piedrahita, J. A., Oetama, B., Bennett, G. D., van Waes, J., Kamen, B. A., Richardson, J., Lacey, S. W., Anderson, R. G. and Finnell, R. H. (1999). Mice lacking the folic acid-binding protein Folbp1 are defective in early embryonic development. *Nat. Genet.* **23**, 228-232.

Saito, A., Pietromonaco, S., Loo, A. K. and Farquhar, M. G. (1994). Complete cloning and sequencing of rat gp330/"megalin," a distinctive member of the low density lipoprotein receptor gene family. *Proc. Natl. Acad. Sci. USA* **91**, 9725-9729.

Spiegelstein, O., Eudy, J. D. and Finnell, R. H. (2000). Identification of two putative novel folate receptor genes in humans and mouse. *Gene* **258**, 117-125.

Spiegelstein, O., Mitchell, L. E., Merriweather, M. Y., Wicker, N. J., Zhang, Q., Lammer, E. J. and Finnell, R. H. (2004). Embryonic development of folate binding protein-1 (Folbp1) knockout mice: Effects of the chemical form, dose, and timing of maternal folate supplementation. *Dev. Dyn.* **231**, 221-231.

Spoelgen, R., Hammes, A., Anzenberger, U., Zechner, D., Andersen, O. M., Jerchow, B. and Willnow, T. E. (2005). LRP2/megalin is required for patterning of the ventral telencephalon. *Development* **132**, 405-414.

Tang, L. S. and Finnell, R. H. (2003). Neural and orofacial defects in Folp1 knockout mice [corrected]. (corrected). *Birth Defects Res. A Clin. Mol. Teratol.* **67**, 209-218.

Travers, D. A. and Haas, S. W. (2004). Evaluation of emergency medical text processor, a system for cleaning chief complaint text data. *Acad. Emerg. Med.* **11**, 1170-1176.

Wallingford, J. B., Niswander, L. A., Shaw, G. M. and Finnell, R. H. (2013). The continuing challenge of understanding, preventing, and treating neural tube defects. *Science* **339**, 1222002.

Willnow, T. E., Hilpert, J., Armstrong, S. A., Rohlmann, A., Hammer, R. E., Burns, D. K. and Herz, J. (1996). Defective forebrain development in mice lacking gp330/megalin. *Proc. Natl. Acad. Sci. USA* **93**, 8460-8464.

Zhao, R., Russell, R. G., Wang, Y., Liu, L., Gao, F., Kneitz, B., Edelmann, W. and Goldman, I. D. (2001). Rescue of embryonic lethality in reduced folate carrier-deficient mice by maternal folic acid supplementation reveals early neonatal failure of hematopoietic organs. *J. Biol. Chem.* **276**, 10224-10228.
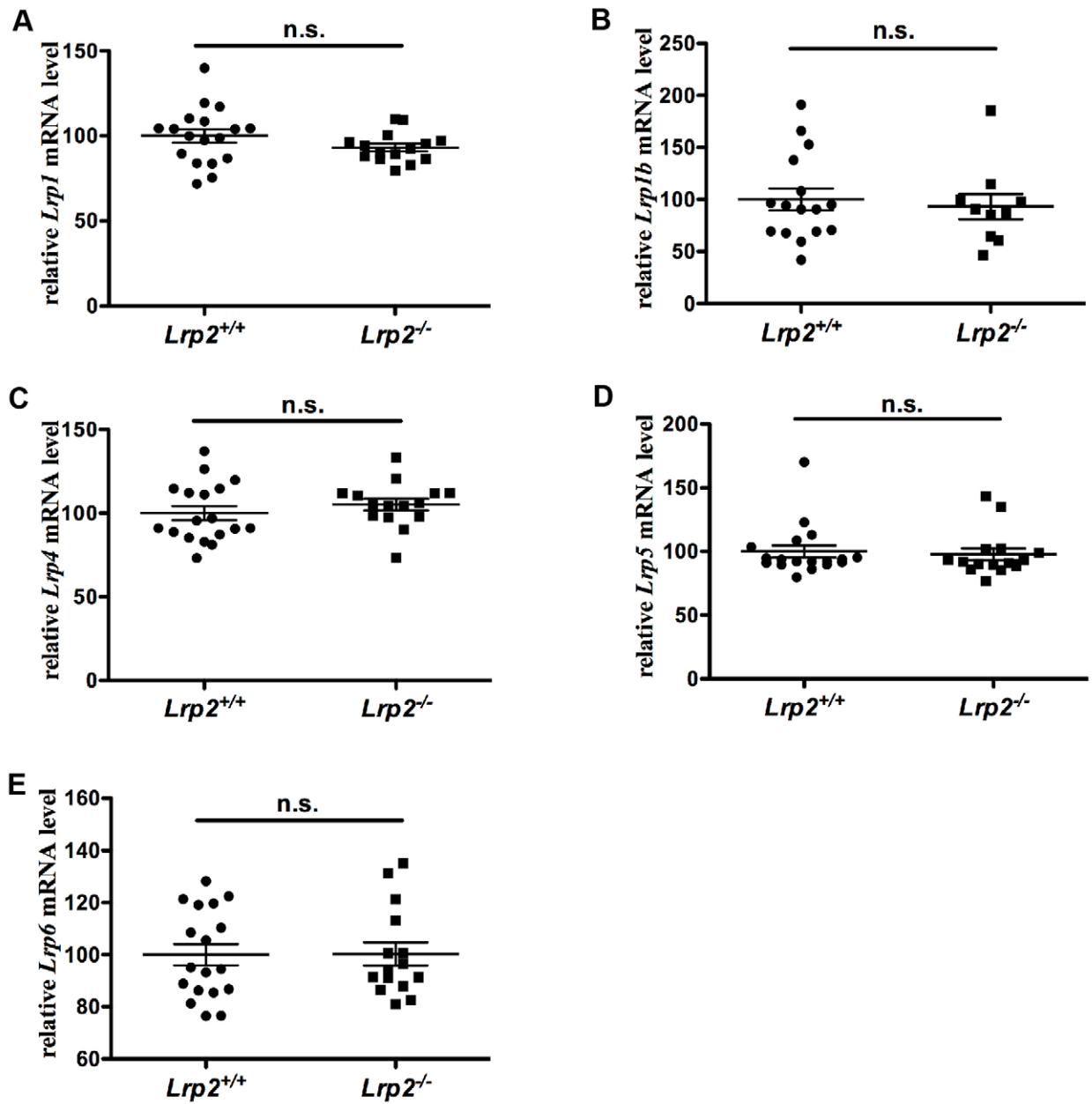
Fig. S1. Expression levels of LDL receptor family members in *Lrp2$^{-/-}$* embryos compared to wild type controls. Quantitative RT-PCR on E9.5 head samples revealed no difference in the expression levels between genotypes for *Lrp1* (A), *Lrp1b* (B), *Lrp4* (C), *Lrp5* (D), and *Lrp6* (E).
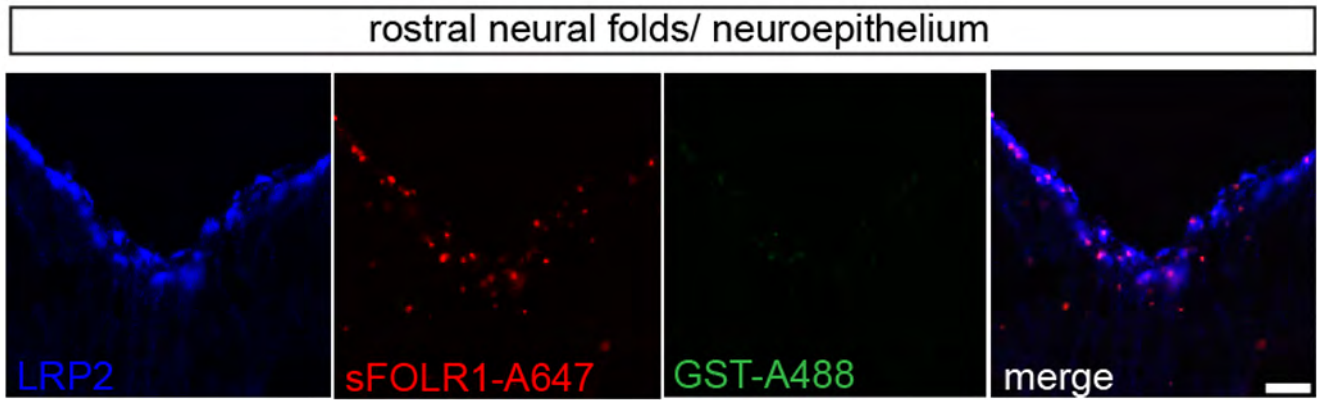
Fig. S2. sFOLR1 uptake experiments in whole embryo cultures. Immunohistological detection of LRP2 (blue) and sFOLR1-A647 (red) on coronal sections of E8.5 whole embryo cultures incubated with sFOLR1-A647 and glutathione S-transferase (GST)-A488. sFOLR1-A647 was internalized whereas no uptake of GST-A488 was seen in the neuroepithelium of control mice (*n*=7). Coronal sections of rostral neural folds, scale bar=10 µm.
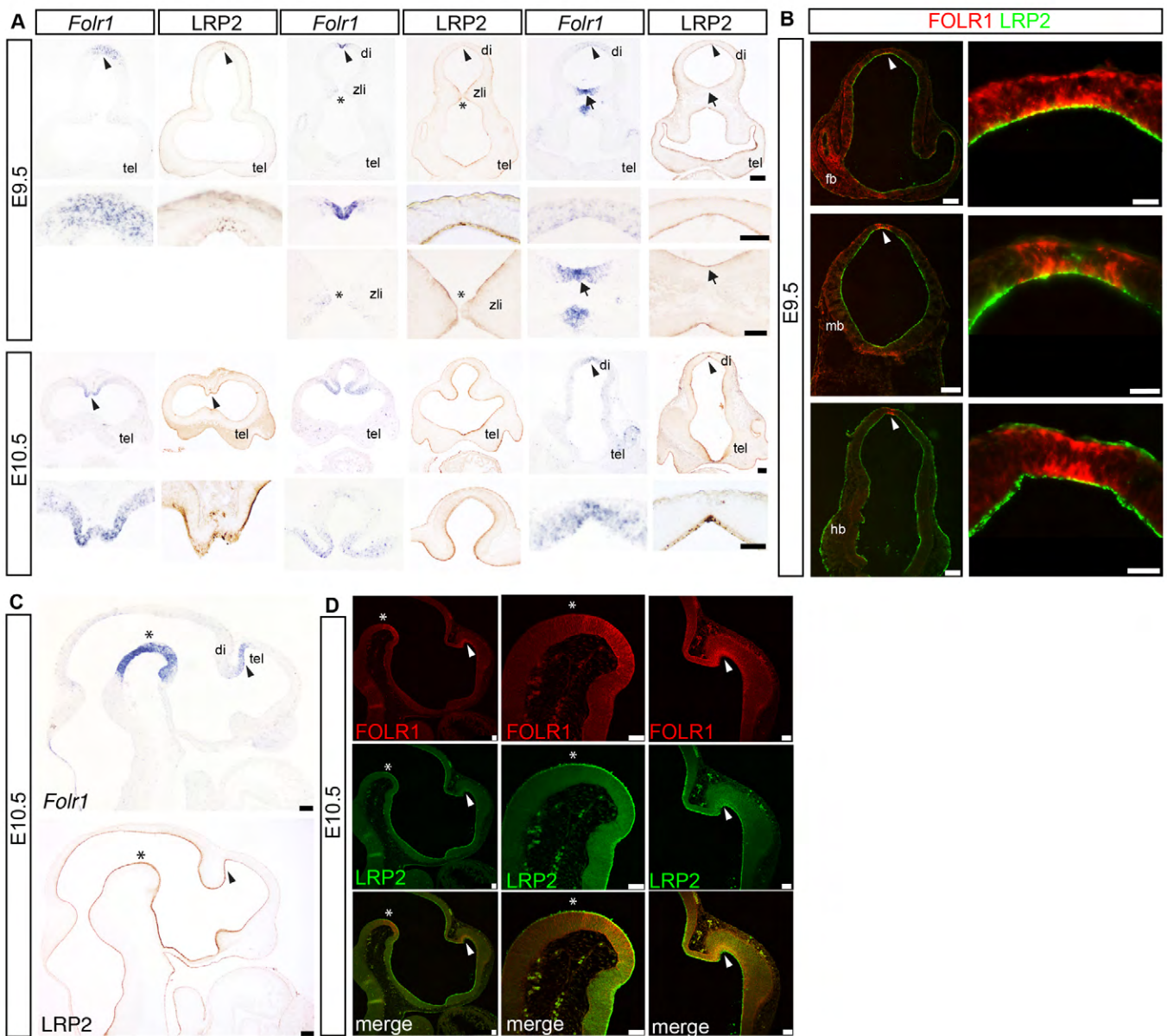
 Fig. S3. FOLR1 and LRP2 expression pattern in the developing neural tube. (A) *Folr1 in situ* hybridization, and immunohistological detection of LRP2 on serial coronal paraffin sections of E9.5 and E10.5 embryonic heads. At E9.5 and E10.5 regions with *Folr1* expression and LRP2 localization on the neighbouring section correspond to the dorsal midline of the telencephalon (tel) and diencephalon (di) indicated by arrowheads, to the zona limitans intrathalamica (zli) indicated by the asterisks, and to the ventral midbrain (arrow). The upper rows for zE9.5 and E10.5, respectively, show the whole coronal head section (scale bar=100 µm). The two lower rows show details of these sections at higher magnification (scale bars=50 µm). (B) Immunohistological detection of FOLR1 (red) and LRP2 (green) on coronal cryostat sections of the forebrain (fb), midbrain (mb), and hindbrain (hb) at E9.5 (scale bars 100 µm). Overlapping signals for FOLR1 and LRP2 are seen in the apical compartment of the neuroepithelial monolayer at the dorsal midline. The right panel presents higher magnification details of the dorsal midline (scale bars=25 µm). (C) *Folr1 in situ* hybridization and immunohistological detection of LRP2 on neighbouring sagittal paraffin sections of E9.5 and E10.5 embryonic heads. Dorsal forebrain (arrowhead) and ventral midbrain (asterisk) show *Folr1* expression and LRP2 localization (scale bars=100 µm). (D) Immunohistological detection of FOLR1 (red) and LRP2 (green) on sagittal brain paraffin sections of E10.5 embryos with overlapping signals for FOLR1 and LRP2 in the dorsal forebrain (arrowhead) and the ventral midbrain (asterisk). Both panels to the right represent higher magnification details of the sagittal sections in the left panel (scale bars=50 µm).